

Possible Non-Perturbative corrections to Bulk Reconstruction

M.Sc Thesis

By
Abhay Kumar Singh



DEPARTMENT OF PHYSICS
INDIAN INSTITUTE OF TECHNOLOGY INDORE
MAY 2025

Possible Non-Perturbative corrections to Bulk Reconstruction

A Thesis

*Submitted in partial fulfillment of the
requirements for the award of the degree*

of

Master of Science

By

Abhay Kumar Singh



DEPARTMENT OF PHYSICS
INDIAN INSTITUTE OF TECHNOLOGY INDORE

MAY 2025



INDIAN INSTITUTE OF TECHNOLOGY INDORE

Candidate declaration

I hereby certify that the work which is being presented in the thesis entitled “**Possible Non-Perturbative Corrections to Bulk Reconstruction**”; in the partial fulfillment of the requirements for the award of the degree of MASTER OF SCIENCE and submitted in the DEPARTMENT OF Physics, Indian Institute of Technology Indore is an authentic record of my own work carried out during the time period from July 2023 to May 2025 under the supervision of Dr. Debajyoti Sarkar, Associate Professor at Indian Institute of Technology Indore. The matter presented in this thesis has not been submitted by me for the award of any other degree of this or any other institute.

Abhay
21/05/25

Signature of the student with date
(Abhay Kumar Singh)

This is to certify that the candidate's above statement is correct to the best of my/our knowledge.

Dr. Debajyoti Sarkar 21/05/25

Signature of the supervisor with date
(Dr. Debajyoti Sarkar)

Abhay Kumar Singh has successfully given his/her M.Sc. Oral Examination held on 13th of May 2025.

Dipankar Das

02-06-25

Signature of the DPGC Physics with date
(DPGC Physics)

ACKNOWLEDGEMENT

I would like to express my sincere gratitude to my supervisor, Dr. Debajyoti Sarkar, for his invaluable guidance, feedback, and support throughout my research. His extensive knowledge and experience were instrumental in the completion of my dissertation.

I am also extremely thankful, to my lab members especially Mirthunjay Nath Bhaiya, for his insightful suggestions and for teaching me multiple mathematical tricks to progress my work, in a similar manner I would like to thank Riskrith on helping me work on this project side by side.

My special thanks go to my dear friends Priyanshu and Namit, who supported me throughout this journey and took care of me as if I were their kin, this would not have been successful without your support.

Last but not least I want to thank my parents for always supporting my dreams and believing in me without a shadow of a doubt that I would pull through. Thank you for your unconditional and unwavering support.

Abstract

It was shown by Kabat and Lifschytz that black holes with finite entropy have their correlation functions of semiclassical bulk operators close to the horizon deviate from their semi-classical values and are ill-defined inside the horizon. This, they argue is due to the behavior of the large-time behavior of the unitary CFT, and means that the region near and inside the horizon receives correction, to that end they propose a cut-off on the boundary CFT as t_{cutoff} which would regulate and ensure that the correlators are well behaved up to a certain point in time. This is done in an ad-hoc manner and it is this prescription that we want to highlight and give a more natural interpretation and manifestation to by using the wormhole metric.

We think that the corrections required for finite N theories could be weaved into the geometry of space-time itself by using this metric, to that extent we hope to recover the results that are central to the ad-hoc time t_{cutoff} that was put in place before by Kabat and Lifschytz.

Thus in the thesis below we define and recover how the worm-hole metric imposes a natural cutoff in the boundary CFT which is symmetric, preserving the light-cone structure, we also derive the bulk to the boundary correlator and match their behavior with what Kabat and Lifschytz have in their work to validate the conjecture and propose the worm-hole as an alternate to the t_{cutoff} prescription.

To achieve this, we re-derive all the results that they have had and thus learn of the procedure required to tackle such a problem. This will help us in the long run when we introduce the modified metric into the problem statement. By drawing parallels, we aim to provide a more natural explanation for the t_{max} cutoff—typically introduced ad hoc in these correlators—within the HKLL framework.

Table of Contents

Table of Contents	iv
1 Introduction	1
1.1 HKLL Prescription	1
1.2 Finite N	2
1.2.1 Eternal-AdS Black Holes	3
2 Analytic calculations for AdS_2 Rindler	8
2.1 HKLL prescription	8
2.2 Excision Process	12
2.3 Correlator Calculation	17
3 Building finite N corrections to HKLL	19
3.1 Wormhole Metric	19
3.2 Solving for the field in AdS_2	20
3.2.1 Sanity Check with known results	22
3.2.2 Finding the normalizable piece for Massive fields for $\lambda = 0$	24
3.3 Massless fields for $\lambda = 0$	25
4 An Analytic journey through the wormhole metric	26
4.1 Bulk reconstruction	26
4.2 Estimation of λ	28
4.3 Correlator	31
5 Future Outlook and Conclusion	32
5.1 Conclusion	32
5.2 Future Outlook	33

Chapter 1

Introduction

Here, we shall go over a brief overview of the motivation behind the problem statement. Furthermore, we shall introduce the HKLL prescription of moving a bulk field $\phi(z, x)$ to its corresponding boundary operator \mathcal{O} using a kernel K . This is then followed by the finite N corrections to the bulk reconstruction in the context of eternal AdS black holes as the theory becomes non-perturbative and thus each term becomes equally important which leads to some rather interesting behavior in the CFT correlators at large time t .

1.1 HKLL Prescription

The Anti-de Sitter/Conformal Field Theory (AdS/CFT) correspondence tells us that any excitation in the bulk is properly encapsulated on the boundary by some operator or state in the CFT (in its Lorentzian version). It is paramount to note that the behavior of such a correspondence is well understood in the semi-classical limit N and large 't Hooft coupling, where it is expected to have free local fields in the bulk, these are encoded in the CFT. Consider a field in the bulk with some normalizable fall-off at the boundary of the AdS.

$$\phi(x, z) \approx z^\Delta \phi_0(x) \tag{1.1}$$

here z is the coordinate with regards to which the bulk field vanishes at the boundary. General AdS/CFT correspondence implies that the boundary behavior of the field corresponds to an operator having the conformal dimension Δ in the CFT.

$$\phi_0(x) \leftrightarrow \mathcal{O}(x) \tag{1.2}$$

This specifies the relation between local fields and non-local operators in the CFT.

$$\phi(z, x) \leftrightarrow \int dx' K(x|z, x) \mathcal{O}(x') \tag{1.3}$$

Thus we may define $K(x'|z, x)$ as a smearing function and hence the bulk-to-bulk correlation is equivalent to the correlation functions of the corresponding non-local operators in the dual CFT. [\[1\]](#)

$$\langle \phi(z_1, x_1) \phi(z_2, x_2) \rangle = \int dx'_1 dx'_2 K(x'_1|z_1, x_1) K(x'_2|z_2, x_2) \langle \mathcal{O}(x'_1) \mathcal{O}(x'_2) \rangle \quad (1.4)$$

To understand the Lorentzian AdS/CFT, the smearing functions must be studied in great detail. They define a map in the semiclassical limit that takes us from the local excitations in the bulk to the operators or states in the boundary that encode them. This semiclassical limit enforces a tight constraint on the finite N behavior. Furthermore, it is important to recognize and stress that smearing functions are not necessarily unique. In some cases, the boundary fields do not have a complete set of Fourier modes and we are thus free to add to the smearing function terms that integrate to zero against all boundary fields. We may exploit this freedom to present the smearing function in different forms as motivated by aspects of what one wishes to study.

A direct example of this arises when computing the smearing function in Rindler coordinates. In this case, constructing the smearing function requires analytically continuing the spatial coordinates of the boundary theory into the complex plane. This mathematical procedure enables us to determine a smearing function that remains supported within a compact region of the corresponding complexified geometry.

1.2 Finite N

The HKLL prescription described above pertains to Bulk Reconstruction in the limit where N is very large or infinite. In this regime, the state operators in the boundary theory define a free local bulk field under the large N limit. Since the Planck length approaches zero ($l_{\text{Planck}} \rightarrow 0$), classical supergravity remains a valid approximation. The construction of operators through the mode sum expansion of the bulk field, evaluated at the boundary, explicitly ensures that the two-point function of these CFT operators reproduces the bulk two-point function.

For finite N in the CFT, any attempt to construct local bulk quantum fields fails. This corresponds to a finite Planck length in the bulk, where the CFT possesses fewer degrees of freedom due to the entropic bound inherent in holographic theories [\[2\]](#). The reduction in degrees of freedom presents a fundamental obstacle, preventing the definition of a truly local bulk field. [\[3\]](#)

Although bulk microcausality can be preserved to all orders in the $\frac{1}{N}$ expansion for large N , at finite N , non-perturbative effects in the CFT—beyond the $\frac{1}{N}$ expansion—lead to violations of microcausality, even in pure AdS. To explore this issue further, it is useful to

consider a background with saturated holographic entropy, such as a black hole spacetime.

1.2.1 Eternal-AdS Black Holes

To understand bulk observables in an AdS-Schwarzschild background, we examine the results of [4]. Specifically, consider a bulk field ϕ positioned just outside the horizon of an Eternal-AdS black hole. This field can be expressed either as a mode sum expansion or as a superposition of CFT operators distributed over the boundary using the smearing function method, valid to all orders in $\frac{1}{N}$.

Although these bulk fields maintain microcausality at each order in $\frac{1}{N}$, this consistency is lost when finite N effects come into play. In particular, the limited entropy of the CFT introduces a constraint that prevents the enforcement of microcausality across the entire bulk. Moreover, as the bulk point approaches the black hole horizon, the corresponding smearing region on the boundary extends infinitely into the future.

To gain deeper insight into this, let us examine correlation functions. Consider a bulk-boundary correlator where the bulk point of interest is positioned just outside the black hole horizon, while the boundary points can be located at any finite time without restriction. This correlator can be represented as a sum of smeared CFT correlators, valid at all orders in the semiclassical approximation.

Now, if we take the limit where the bulk point approaches the future horizon, we observe that the corresponding smearing region on the boundary extends indefinitely into the future. This indicates that the correlator is increasingly influenced by the late-time behavior of CFT correlators. At finite entropy, this behavior becomes highly intricate and is determined by the spectrum of the CFT state at the boundary. Consequently, bulk field observables near the horizon become fine-grained and sensitive to the black hole's microstate. As a result, the semiclassical approximation breaks down in the vicinity of the horizon.

At late times and finite temperatures, CFT correlation functions exhibit exponential decay, as demonstrated by the following relation.

$$\langle \mathcal{O}(t)\mathcal{O}(0) \rangle \approx e^{\frac{-2\pi\Delta t}{\beta}} \quad (1.5)$$

where β encodes the periodicity in imaginary time. This behavior may be understood as the result of dissipating excitations into an infinite heat bath. However such exponential

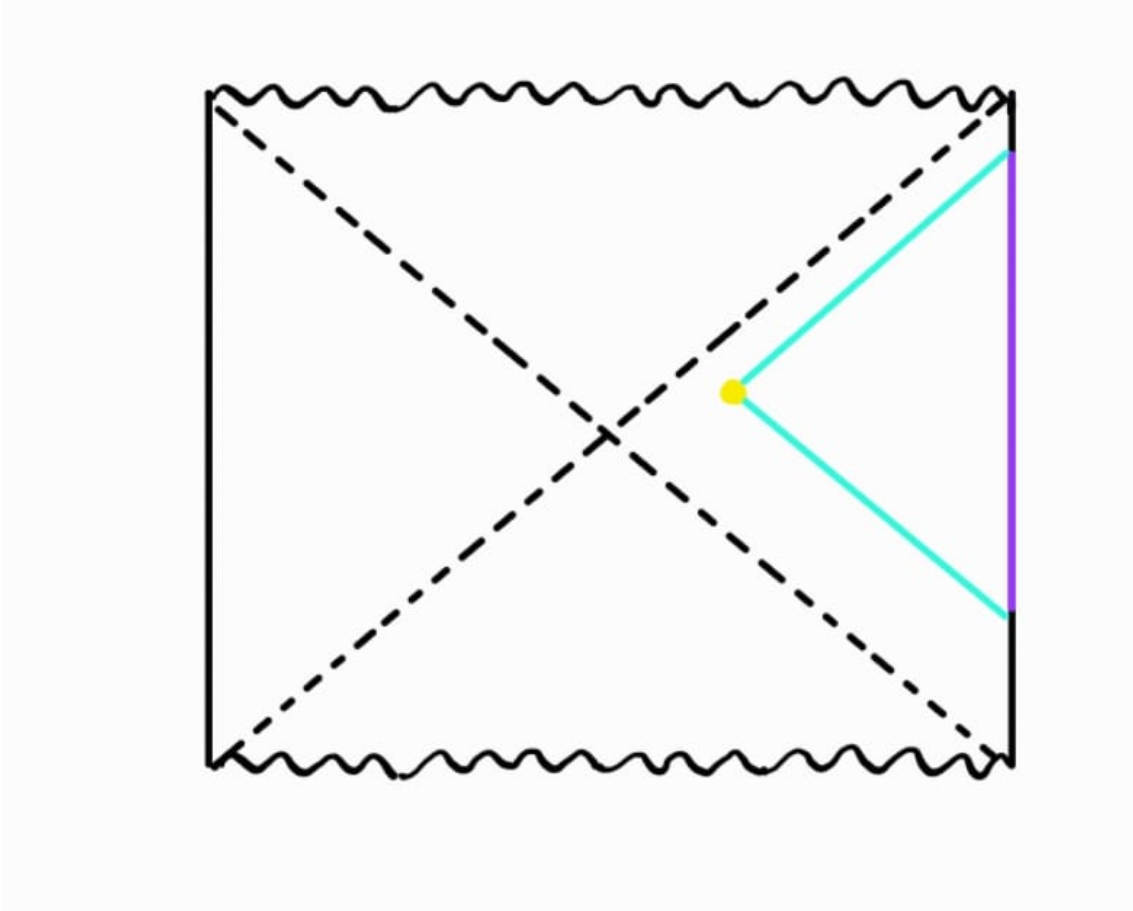


Figure 1.1: An AdS-Schwarzschild black hole with a bulk field operator inserted outside the horizon. To all orders in $\frac{1}{N}$, the bulk field can be represented as a sum of CFT operators. The CFT operators are smeared over a region of the complexified boundary (indicated in purple) which is spacelike separated from the bulk point (indicated in yellow).

decay cannot continue indefinitely in a system with only finite entropy. Instead, there exists a lower bound beyond which the correlator cannot decay i.e. below the inner product of the two normalized vectors in the Hilbert space of the given system. We see that on random if we pick two unit vectors then on an average.

$$|\langle \psi_1 | \psi_2 \rangle| \approx \frac{1}{\sqrt{\dim \mathcal{H}}} = e^{-\frac{S}{2}} \quad (1.6)$$

where S is the entropy. The pictorial representation of such a process is sketched below, The exponential decay of the correlators occurs up to a time t_{max} . After t_{max} , fluctuations of size set by $e^{-\frac{S}{2}}$ is exhibited by the correlator hence we see that

$$t_{max} = \frac{\beta S}{4\pi\Delta} \quad (1.7)$$

To summarize the key idea, after a time t_{max} , the system begins to recognize that it exists within a finite-dimensional Hilbert space. It takes a much longer duration, known as the

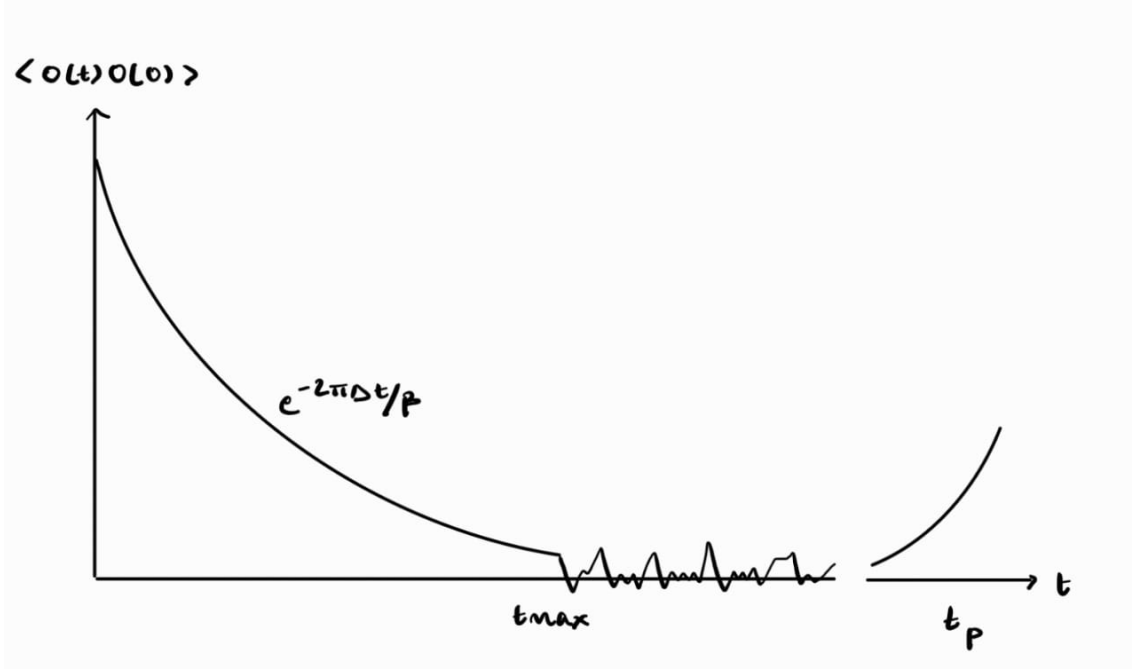


Figure 1.2: A sketch of a CFT correlator in a generic pure state shows an initial exponential decay up to t_{max} , after which it begins to fluctuate. Eventually, after the Poincaré time, the correlator undergoes a large

Heisenberg time $t_H \approx \beta e^S$, for the system to fully identify its specific microstate. Beyond the Poincaré time $t_P \approx \exp(e^S)$, the correlator starts exhibiting significant fluctuations.

At late times, correlators in a finite-entropy system do not simply decay exponentially but instead experience fluctuations, complicating the definition of bulk observables. The $\frac{1}{N}$ expansion represents bulk fields as integrals over spacelike-separated boundary points, with support extending over a certain region. As previously discussed, when the bulk point nears the horizon, this integration region stretches to infinite time. In the semiclassical approximation, the scenario remains manageable because correlators at infinite N decay exponentially without end, effectively counteracting the divergence in entropy. However, at finite N , correlators stop decaying past t_{max} . Instead, as the smearing region extends to t_{max} , the bulk correlators cease to be smooth functions of position and begin fluctuating indefinitely with fluctuations of order $e^{-\frac{S}{2}}$. Additionally, at very late times, larger fluctuations emerge due to the long-time behavior of the CFT correlators. This outcome deviates from what one would expect based on semiclassical intuition. Moreover, this behavior makes bulk observables ill-defined as they approach the horizon.

For bulk points inside the horizon, the issue becomes even more severe. The semiclassical smearing function grows exponentially with time, and when integrated with the fluctuating CFT correlator, the resulting expression becomes nonsensical.

At this point, one might be inclined to conclude that bulk physics near and inside the horizon is inherently ill-defined. However, before arriving at such a conclusion, it is important to recall that in the holographic framework, the boundary CFT is considered fundamental, with bulk physics emerging from it. This perspective allows us to construct an approximate description of bulk physics in terms of the CFT. A crucial question then arises: Can bulk observables be meaningfully defined solely within the CFT framework? Such observables should remain well-behaved both near and potentially inside the horizon while still reproducing semiclassical physics with only small corrections.

A well-defined approach exists for constructing the bulk field in an AdS-Schwarzschild black hole, enabling the placement of an operator near or even inside the horizon. Given the non-uniqueness of the smearing function, the problematic late-time region can be removed to regulate its behavior. By excluding this troublesome region, we can continue using the semiclassical expression for the bulk field in terms of the CFT.

By introducing a cutoff at t_{max} , we ensure that integration on the boundary never extends beyond $t = t_{max}$, thereby avoiding the emergence of ill-defined bulk physics. For bulk points inside the horizon, the corresponding smearing functions are expected to receive contributions from both boundaries. Consequently, we must also excise the regions near both future and past infinities to maintain a well-behaved formulation, as illustrated below.

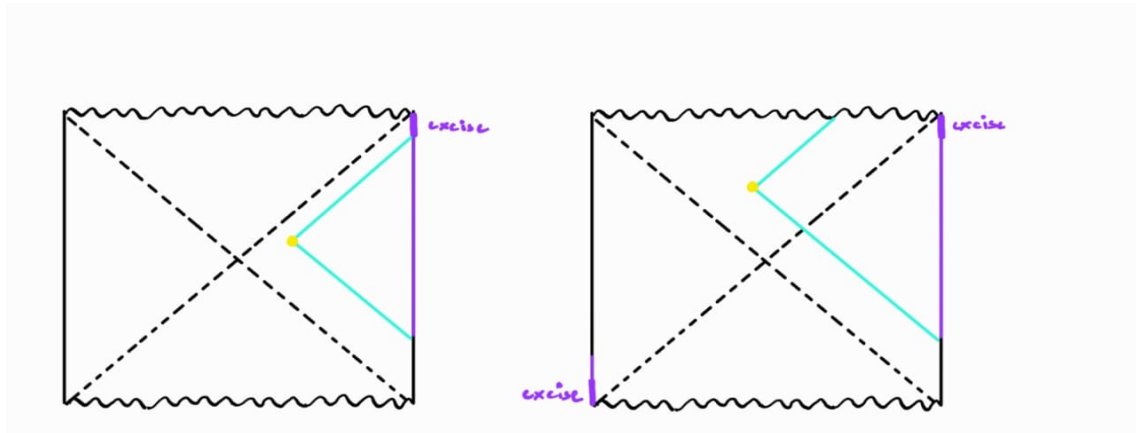


Figure 1.3: On the left, an AdS-Schwarzschild black hole with a bulk field operator inserted outside the horizon. The purple region is excluded from the smearing function. On the right, when the bulk point lies inside the horizon, we expect the smearing function to have support on both boundaries.

The reasoning outlined above, where an ad-hoc modification is introduced, can be directly interpreted as an adjustment to the definition of a bulk operator. Specifically, this involves modifying the CFT correlation function by discarding the component that

depends on the finite entropy structure and, consequently, the microstate of the CFT. In essence, this process "coarse-grains" the relevant portion of the CFT, allowing us to recover a well-behaved—though approximate—description of bulk physics, whether near or inside the horizon.

This idea is particularly significant in the context of this report, as it serves as a pivotal point leading to the conjecture we will present later. It also aligns well with an alternative approach we may consider for incorporating non-perturbative corrections into bulk reconstruction.

Furthermore, to clarify the cutoff procedure, it is essential to recognize that, based on the uncertainty principle, imposing a time cutoff t_{max} corresponds to limiting the resolution of energy measurements.

$$\Delta E \approx \frac{1}{t_{max}} \approx \frac{1}{\beta S} \quad (1.8)$$

Introducing a time cutoff effectively results in averaging over CFT microstates whose energy differences are smaller than ΔE . This process can be related to the energy fluctuations that naturally arise in the canonical ensemble, where such variations are dictated by the specific heat. In a CFT, the specific heat is directly proportional to the system's entropy.

$$\Delta E_{canonical} = \frac{1}{\beta} \sqrt{c} \approx \frac{1}{\beta} \sqrt{S} \quad (1.9)$$

As a result, the cutoff procedure enables energy resolutions that are significantly more refined than the fluctuations typically found in the canonical ensemble. The key advantage of this approach is that it effectively eliminates the problematic late-time behavior of the CFT correlator. This, in turn, allows us to reconstruct an approximate description of bulk physics—something that would not be achievable by simply averaging over microstates.

Chapter 2

Analytic calculations for AdS_2 Rindler

Having built all of the intuition required to understand the HKLL treatment of finite N theories, we highlight and show how to derive all these results analytically initially for the original metric, followed by the wormhole metric. The calculation done for these sections will employ the usage of a coordinate transformation known as the “tortoise coordinate”. The motivation here is to learn the technique and mathematical skills employed by Kabat and Lifschytz in their paper “Finite N and the failure of bulk locality: Black holes in AdS/CFT ”. This would allow us to apply a similar analysis for the wormhole metric which we hope weaves in the finite N corrections into the geometry of space-time itself. An important aspect of this calculation is to note that the analysis here is done for a Rindler horizon as the fluctuations one might expect will be absent as the entropy is infinite. Regardless, the study would help us understand how the field’s excision occurs near the late-time region near the horizon. Furthermore, we may later work on the AdS_3 blackhole and recover the said fluctuations near time $t = t_{max}$ on the image sum in the periodic coordinate of the blackhole and subsequently apply this very same formalism of modifying the metric for that case as well and recovering the finite N corrections and the t_{cutoff} in a more natural manner than what was specified by Kabat and Lifschytz.

2.1 HKLL prescription

$$ds^2 = -\frac{r^2 - r_h^2}{R^2} dt^2 + \frac{R^2}{r^2 - r_h^2} dr^2 \quad (2.1)$$

In the KL paper, we have: $r_h = R$ therefore the metric becomes

$$\begin{aligned} ds^2 &= -\frac{r^2 - R^2}{R^2} dt^2 + \frac{R^2}{r^2 - R^2} dr^2 \\ ds^2 &= \Omega^2(r) [-dt^2 + dr^{*2}] \end{aligned} \quad (2.2)$$

where,

$$\begin{aligned} dr^* &= \frac{R^2}{r^2 - R^2} dr \\ dr^* &= \frac{1}{\frac{r^2}{R^2} - 1} dr \end{aligned} \quad (2.3)$$

Let us make the following substitution:

$$\begin{aligned} \coth u &= \frac{r}{R} \\ -\csc^2 u \, du &= \frac{dr}{R} \end{aligned} \quad (2.4)$$

We know,

$$\coth^2 u - 1 = \csc^2 u \quad (2.5)$$

Therefore,

$$\begin{aligned} r^* &= - \int \frac{R \csc^2 u}{\coth^2 u - 1} du \\ &= -R \int du \\ &= -Ru + c \quad \text{set } c \rightarrow 0 \end{aligned} \quad (2.6)$$

Hence for the appropriate set of limits for r , we see that as $r \rightarrow R$;

$$u = \coth^{-1} 1 = \infty \quad (2.7)$$

For $r \rightarrow \infty$

$$u = \coth^{-1} \infty = 0 \quad (2.8)$$

Hence we see that r^* has the value

$$\begin{aligned} r^{*2} &= -R \coth^{-1} \frac{r}{R} \\ &= -\frac{R}{2} \log \frac{r+R}{r-R} \end{aligned} \quad (2.9)$$

Let us now find the Kernel using the mode sum approach as prescribed by HKLLcite. The field is given by solving the Klien Gordon Equation.

$$\frac{1}{\sqrt{-g}} \partial_\mu [\sqrt{-g} g^{\mu\nu} \partial_\nu \Phi] = 0 \quad (2.10)$$

For the given metric, Klien Gordon gives us the following solution for the field:

$$\Phi(r, t) = C_1 \cos \omega r^* e^{-i\omega t} + C_2 \sin \omega r^* e^{-i\omega t} \quad (2.11)$$

Now to find the normalizable piece we must analyze the field at the boundary i.e. $r \rightarrow \infty$. The condition is that the field piece must vanish as $r^{-\Delta}$ at the boundary.

Therefore,

$$\lim_{r \rightarrow \infty} \Phi(r, t) = C_1 \left(1 - \frac{R^4 \omega^2}{2r^2} \right) + C_2 \left(-\frac{R^2 \omega}{r} \right) \quad (2.12)$$

We see that at $r \rightarrow \infty$ it is the sin term that has a normalizable fall off hence we may write:

$$C_2 \left(\frac{R^2}{r} \right)^\Delta (-\omega^2) \quad (2.13)$$

Here, $\Delta = 1$; In the Rindler co-ordinates we may take the following to be the normalization:

$$\Phi(r, t) \approx \left(\frac{R^2}{r} \right)^\Delta \phi_0(t) \quad \text{as } r \rightarrow \infty \quad (2.14)$$

Therefore,

$$C_2 \left(\frac{R^2}{r} \right) (-\omega^2) = \left(\frac{R^2}{r} \right) a_\omega \quad (2.15)$$

$$C_2 = -\frac{a_\omega}{\omega}$$

Now, we may write the mode sum for the field which will be:

$$\begin{aligned} \Phi(r, t) &= \frac{1}{\sqrt{2\pi}} \int_{-\infty}^{\infty} d\omega \left(e^{-i\omega t} f_\omega(r) \frac{a_\omega}{\omega} + h.c \right) \\ &= \frac{1}{\sqrt{2\pi}} \int_{-\infty}^{\infty} \int_{-\infty}^{\infty} dt d\omega \left(e^{-i\omega(t-t')} \sin \left(\frac{\omega R}{2} \log \frac{r+R}{r-R} \right) \frac{O(t')}{\omega} + h.c \right) \end{aligned} \quad (2.16)$$

Therefore, the Kernel is given by:

$$K(r, t) = \frac{1}{2\pi} \int_{-\infty}^{\infty} \frac{d\omega}{\omega} e^{-i\omega(t-t')} \sin \left(\frac{\omega R}{2} \log \frac{r+R}{r-R} \right) \quad (2.17)$$

For a compact calculation let us work with r^* instead.

$$K(r, t) = \frac{1}{2\pi} \int_{-\infty}^{\infty} \frac{d\omega}{\omega} e^{-i\omega(t-t')} \sin \omega r^* \quad (2.18)$$

Using the Euler identity for the sin term we have:

$$\sin \omega = \frac{e^{(i\omega r^*)} - e^{-i\omega r^*}}{2i} \quad (2.19)$$

Therefore now the integral becomes

$$\begin{aligned} I &= \frac{1}{4\pi i} \int_{-\infty}^{\infty} \frac{d\omega}{\omega} e^{-i\omega(t-t')} (e^{(i\omega r^*)} - e^{-i\omega r^*}) \\ I &= \frac{1}{4\pi i} \int_{-\infty}^{\infty} \frac{d\omega}{\omega} (e^{-i\omega(t-t'-r^*)} - e^{-i\omega(t-t'+r^*)}) \end{aligned} \quad (2.20)$$

Now we shall use the following identity for the Signum function using the Fourier transform:

$$\begin{aligned}
F[Sgn(x)](\omega) &= \frac{2}{i\omega} \\
F^{-1}[Sgn(x)](\omega) &= Sgn(x) \\
\frac{1}{2\pi} \int_{-\infty}^{\infty} \frac{e^{i\omega x}}{\omega} dx &= i\pi Sgn(x) \\
\frac{1}{2\pi} \int_{-\infty}^{\infty} \frac{e^{-i\omega x}}{\omega} dx &= -i\pi Sgn(x) \text{ **complex conjugate** }
\end{aligned} \tag{2.21}$$

Using this identity in (2.20) we get

$$\begin{aligned}
I &= \frac{1}{4\pi i} [-i\pi Sgn(t - t' - r^*) + i\pi Sgn(t - t' + r^*)] \\
K(t, r) &= \frac{1}{4} [-i\pi Sgn(t - t' - r^*) + i\pi Sgn(t - t' + r^*)]
\end{aligned} \tag{2.22}$$

Studying the Signum function, as per the definition of the Signum function we have:

$$\begin{aligned}
Sgn(x - a) &= 1 \quad \text{for } x > a \\
Sgn(x - a) &= 0 \quad \text{for } x = a \\
Sgn(x - a) &= -1 \quad \text{for } x < a
\end{aligned} \tag{2.23}$$

Case 1: $t' < (t - r^*)$ the lower limit

$$\begin{aligned}
Sgn[(t + r) - t'] &> 0] = 1 \\
Sgn[(t - r) - t'] &> 0] = 1 \\
Sgn[(t + r) - t'] - Sgn[(t - r) - t'] &= 0
\end{aligned} \tag{2.24}$$

Case 2: $t' \in (t - r, t + r)$ t' belongs within the limits

$$\begin{aligned}
Sgn[(t + r) - t'] &> 0] = 1 \\
Sgn[(t - r) - t'] &< 0] = -1 \\
Sgn[(t + r) - t'] - Sgn[(t - r) - t'] &= 2
\end{aligned} \tag{2.25}$$

Case 3: $t' > (t + r^*)$ the upper limit

$$\begin{aligned}
Sgn[(t + r) - t'] &> 0] = -1 \\
Sgn[(t - r) - t'] &> 0] = -1 \\
Sgn[(t + r) - t'] - Sgn[(t - r) - t'] &= 0
\end{aligned} \tag{2.26}$$

From the above analysis, we see that due to the presence of the $Sgn(x)$ functions the limit of the integral changes from $[-\infty, \infty]$ to $[t + r^*, t - r^*]$ where the $Sgn(x)$ functions add

up when t' lies within the latter values, there for Bulk reconstruction of the Semi-classical field we have:

$$\begin{aligned}\Phi(t, r) &= \int_{-\infty}^{\infty} KO(t') dt' \\ &= \int_{-\infty}^{\infty} \frac{1}{4} [Sgn(t - t' + r^*) - Sgn(t - t' - r^*)] O(t') dt'\end{aligned}\tag{2.27}$$

Therefore using what we have learned the above equation reduces to:

$$\Phi(t, r) = \frac{1}{2} \int_{t-r^*}^{t+r^*} O(t') dt' \tag{2.28}$$

Using the value of r^* we get:

$$\begin{aligned}\Phi(t, r) &= \frac{1}{2} \int_{t-\frac{R}{2} \log \frac{r+R}{r-R}}^{t+\frac{R}{2} \log \frac{r+R}{r-R}} O(t') dt' \\ &= \frac{1}{2} \int_{t-\delta t}^{t+\delta t} O(t') dt'\end{aligned}\tag{2.29}$$

where δt gives us the support spread of the Kernel on the boundary region. Think of light cones being dropped from some bulk point to the boundary at the spatial infinity.

2.2 Excision Process

Next, let us make some concrete comments on the excision process, we may first ask ourselves the question, how close can we reach the horizon before the cut-off makes any difference? Given the spread, let us impose a cut-off time at $t = t_{max}$

From the light-cone relation we have the following:

$$\delta t = \frac{1}{2} R \log \frac{r+R}{r-R} \tag{2.30}$$

At $t = t_{max}$ we have:

$$t_{max} = \frac{R}{2} \log \frac{r+R}{r-R} \tag{2.31}$$

Substituting the value of t_{max} from [\[4\]](#) we have:

$$\begin{aligned}\frac{RS}{2\Delta} &= \frac{R}{2} \log \frac{r+R}{r-R} \\ e^{\frac{S}{2\Delta}} &= \sqrt{\frac{r+R}{r-R}} \\ r &\gtrsim R \left(1 + 2e^{-\frac{S}{\Delta}}\right)\end{aligned}\tag{2.32}$$

Hence from this equation, it is evident that we may go exponentially close to the horizon before the cut-off makes any difference, i.e. before the effects of the finite N corrections come into play.

Let us now perform the excision procedure to get the proper finite N behavior. Thus the modified field for a bulk point near the horizon can be thought to have a cut-off t_{cut} on the boundary support.

$$\Phi_{mod}(t, r) = \frac{1}{2} \int_{t-\delta t}^{t_{cut}} dt' O(t') \quad (2.33)$$

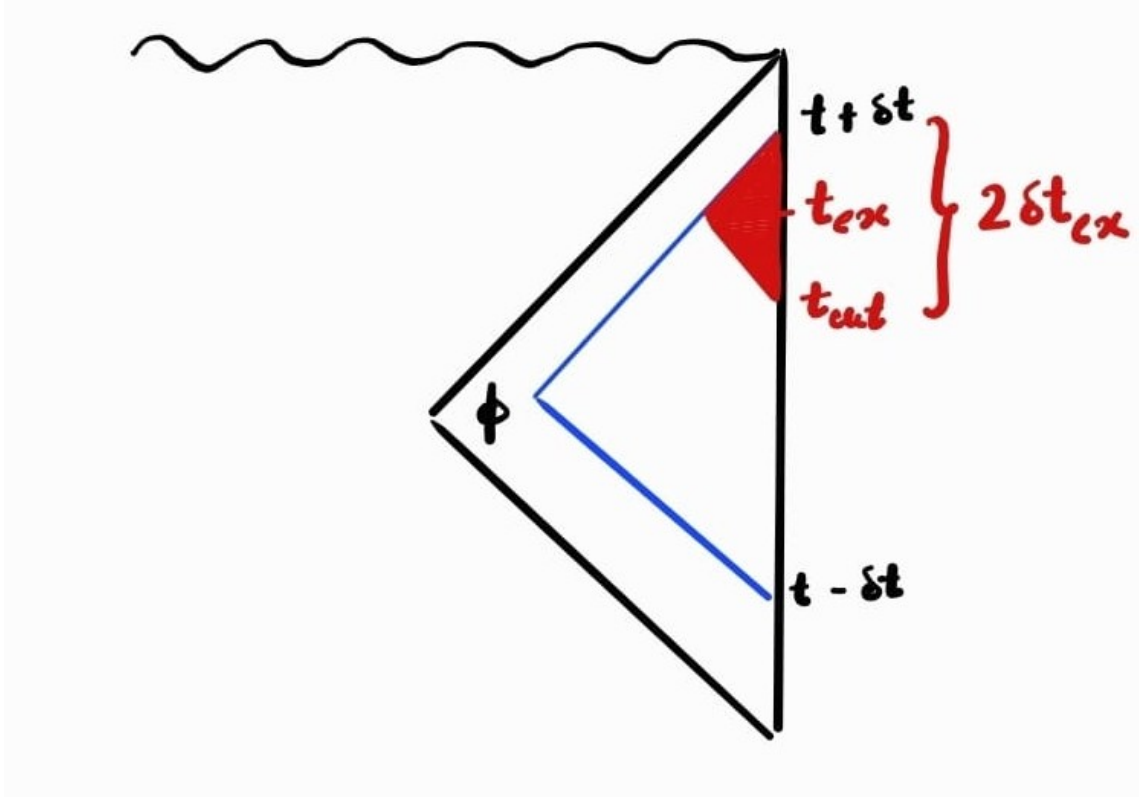


Figure 2.1: The excision of the field is given here in red, which specifies the removal of the late time behavior CFT related bulk points .

The modified field can also be thought of in terms of the following:

$$\begin{aligned} \frac{1}{2} \int_{t-\delta t}^{t_{cut}} O(t') dt' &= \frac{1}{2} \int_{t-\delta t}^{t+\delta t} O(t') dt' - \frac{1}{2} \int_{t_{cut}}^{t+\delta t} O(t') dt' \\ &= \Phi_{semi-classical}(t, r) - \Phi_{semi-classical}(t_{ex}, r_{ex}) \end{aligned} \quad (2.34)$$

Here,

$$\begin{aligned}\Phi_{semi-classical}(t_{ex}, r_{ex}) &= \frac{1}{2} \int_{t_{ex}-\delta t_{ex}}^{t_{ex}+\delta t_{ex}} O(t') dt' \\ t_{ex} &= \frac{t_{cut} + t + \delta t}{2} \\ \delta t_{ex} &= \frac{t + \delta t - t_{cut}}{2} \\ &= t_{ex} - t_{cut}\end{aligned}\tag{2.35}$$

Also by definition we have:

$$\begin{aligned}\delta t &= \frac{R}{2} \log \frac{r+R}{r-R} \\ &= \coth^{-1} \frac{r}{R} \\ r &= R \coth \frac{\delta t}{R}\end{aligned}\tag{2.36}$$

Therefore,

$$\begin{aligned}r_{ex} &= R \coth \frac{\delta t_{ex}}{R} \\ &= R \coth \frac{t + \delta t - t_{cut}}{R}\end{aligned}\tag{2.37}$$

Let us now select a prescription for t_{max} setting as was done by Kabat Lifschytz in their 2014 paper [\[4\]](#).

$$2\delta t_{ex} = t_{max}\tag{2.38}$$

and

$$t_{cut} = t + \delta t - t_{max}\tag{2.39}$$

When $r \approx R$, $t \rightarrow \infty$ in the future late time as $\delta t_{ex} \rightarrow \infty$, making the total range as t_{max} . t_{max} is the total width of the excised boundary region.

To excise the region $t > t_{max}$ from the smearing function of the Bulk operator we switch to the Poincaré coordinates as Rindler coordinates have a coordinate singularity at $t = \infty$. We have shall do this procedure for AdS₃ and then take it down for the 2 dimensional case as was done by KL:

$$\begin{aligned}\Phi(Z_{ex}, T_{ex}) &= \int_{spacelike} K(Z_{ex}, T_{ex}, \vec{X}) O(T', Y') dT' dY' \\ &= \int dT' dY' \left(\frac{Z_{ex}^2 - |\vec{Y}|^2 - (T - T')^2}{2Z_{ex}} \right)^{\Delta-d} O(T + T', X + iY')\end{aligned}\tag{2.40}$$

From the above equation we infer that the Kernel has semblance to the invariant AdS distance formula therefore,

$$\frac{Z_{ex}^2 - |\vec{Y}|^2 - (T - T')^2}{2Z_{ex}} \gtrsim 0\tag{2.41}$$

For, T' near excision $T' = R$; $|\vec{Y}|^2 = 0$; $\hat{\phi} = 0$

$$\begin{aligned} Z_{ex}^2 &\gtrsim (T - R)^2 \\ Z_{ex} &\approx \text{radius of the excised region} \\ &\approx (T - R) \end{aligned} \tag{2.42}$$

Therefore we see that in the Poincare coordinates all of this results in a region/sphere of radius $(T - R)$ being cut out from the entire region. It is a sphere for AdS₃ whereas the area will correspond to a circular region for AdS₂.

Now let us use the embedding coordinates to go between Rindler and Poincaré coordinates.

$$\begin{aligned} u &= \frac{Rr}{r_h} \cosh \frac{r_h \hat{\phi}}{R} \\ v &= R \sqrt{\frac{r^2}{r_h^2} - 1} \sinh \frac{r_h t}{R^2} \\ y &= R \sqrt{\frac{r^2}{r_h^2} - 1} \cosh \frac{r_h t}{R^2} \\ x &= \frac{Rr}{r_h} \sinh \frac{r_h \hat{\phi}}{R} \end{aligned} \tag{2.43}$$

Also in Poincaré coordinates we have:

$$\begin{aligned} u &= \frac{R^2 + Z^2 - T^2 + X^2}{2Z} \\ v &= \frac{RT}{Z} \\ x &= \frac{RX}{Z} \\ y &= \frac{R^2 - Z^2 + T^2 - X^2}{2Z} \end{aligned} \tag{2.44}$$

Using how the embedding coordinates are related to each other in two different coordinate systems, it is rather easy to find a coordinate transformation between the two thus after some algebra we have the following relation:

$$\tanh \frac{t}{R} = \frac{2RT}{R^2 - Z^2 + T^2 - X^2} \tag{2.45}$$

Now towards the future of the AdS₂ at $T \approx R$, $X = 0$, $Z = Z_{ex}$, $\delta t \rightarrow t_{max}$, near the boundary we have:

$$\tanh \frac{t}{R} = \frac{2RT}{R^2 + T^2} \tag{2.46}$$

Using the relation

$$\tanh^{-1} x = \frac{1}{2} \log \frac{1+x}{1-x} \quad (2.47)$$

Therefore we get the following:

$$\tanh^{-1} \frac{2RT}{R^2 + T^2} = \log \frac{T+R}{T-R} \quad (2.48)$$

Taking the limit as $T \rightarrow R$ we essentially have the following $t \rightarrow t_{max}$

$$\begin{aligned} \frac{t_{max}}{R} &\approx \log \frac{2R}{T-R} \\ e^{-\frac{t_{max}}{R}} &= \frac{T-R}{2R} \end{aligned} \quad (2.49)$$

Therefore we may now write Z_{ex} in terms of t_{max} as set in the Rindler coordinates

$$\begin{aligned} Z_{ex} &\approx T - R \\ &\approx 2Re^{-\frac{t_{max}}{R}} \\ &\approx 2Re^{-\frac{S}{2\Delta}} \end{aligned} \quad (2.50)$$

Hence our claim in the equation (2.34) has been validated for massless fields as:

$$\begin{aligned} \Phi_{semi-classical}(Z_{ex}) &= (Z_{ex})^\Delta O(T' = R, X = 0) \\ &= 2Re^{-\frac{S}{2}} O(T = R) \end{aligned} \quad (2.51)$$

Finally, we may write and thus conclude that to a good extent what is actually being excised is an operator in the Poincaré coordinates:

$$\Phi_{mod}(r, t) = \Phi_{semi-classical}(r, t) - 2Re^{-\frac{S}{2}} O(T = R) \quad (2.52)$$

Furthermore, an important note is that the equation (2.34) is valid only for massless fields. When massive fields are considered the excision will not be of such a simple form instead we will have multiple superpositions of various operators that are excised from the bulk field at different small rs and large ts .

For the general $\Delta \neq d$

$$\Phi_{modified} = \Phi_{semiclassical} - e^{-\frac{dS}{2\Delta}} O(T = R) \quad (2.53)$$

Thus at the end of the day, it suffices to agree with what Kabat and Lifschytz have to say about having changed the definition of the bulk field near the Rindler Horizon for finite N cases.

2.3 Correlator Calculation

Let us now calculate the Bulk-Boundary correlator, for this calculation let us use the CFT two-point function.

$$\langle O_R(t)O_R(t') \rangle = \frac{1}{2(1 - \cosh t - t')} \quad (2.54)$$

For a bulk point outside the horizon, we have:

$$\Phi(t, r) = \frac{1}{2} \int_{t-\delta t}^{t+\delta t} dt' O_R(t') \quad (2.55)$$

The range of the smearing function is set by:

$$\delta t = \frac{1}{2} \log \frac{r+1}{r-1} \quad (2.56)$$

This means the bulk-boundary two-point function is:

$$\begin{aligned} \langle \Phi(t, r)O_R(t'') \rangle &= \frac{1}{4} \int_{t-\delta t}^{t+\delta t} \frac{1}{1 - \cosh(t' - t'')} dt' \\ &= -\frac{1}{8} \int_{t-\delta t}^{t+\delta t} \frac{1}{2 \sinh^2(\frac{t'-t''}{2})} dt' \\ &= \frac{1}{4} \left(\coth \frac{t + \delta t - t''}{2} - \coth \frac{t - \delta t - t''}{2} \right) \end{aligned} \quad (2.57)$$

We shall now use the identities

$$\begin{aligned} \frac{1}{4} \left(\coth \frac{A+B}{2} - \coth \frac{A-B}{2} \right) &= \frac{1}{2} \left(\frac{\sinh A}{\cosh B - \cosh A} \right) \\ \cosh^2 A - \sinh^2 A &= 1 \end{aligned} \quad (2.58)$$

Therefore the above equation simplifies to

$$\frac{1}{4} \left(\coth \frac{t + \delta t - t''}{2} - \coth \frac{t - \delta t - t''}{2} \right) = \frac{1}{2} \left(\frac{\sinh \delta t}{\cosh \delta t - \cosh(t - t'')} \right) \quad (2.59)$$

This can be further simplified as,

$$\begin{aligned} \cosh \delta t &= \frac{r}{\sqrt{r^2 - 1}} \\ \sinh \delta t &= \frac{1}{\sqrt{r^2 - 1}} \end{aligned} \quad (2.60)$$

Therefore the correlator takes the form:

$$\langle \Phi(t, r)O_R(t'') \rangle = \frac{1}{2(r - \sqrt{r^2 - 1} \cosh t - t'')} \quad (2.61)$$

Now let us evaluate the correlator with a cut-off in t , thus the modified correlator becomes

$$\langle \Phi(t, r) O_R(t'') \rangle = \frac{1}{4} \int_{t-\delta t}^{t_{cut}} \frac{1}{1 - \text{Cosh}(t' - t'')} dt' \quad (2.62)$$

Kabat and Lifchytz tell us that this is similar to inserting a bulk point at a new position.

$$\begin{aligned} t_{new} &= \frac{t_{cut} + t - \delta t}{2} \\ r_{new} &= \coth \frac{t_{cut} - (t - \delta t)}{2} \end{aligned} \quad (2.63)$$

We may also think of this as excising a $\Phi_{semi-classical}(t_{ex}, r_{ex})$ which has already been shown earlier in the previous section. Thus the correlator for such a field that has been excised is given by:

$$\langle \Phi_{semi-classical}(t_{ex}, r_{ex}) O_R(t'') \rangle = \frac{1}{2(r_{ex} - \sqrt{r_{ex}^2 - 1} \cosh t_{ex} - t'')} \quad (2.64)$$

According to the prescription proposed so far, this is the correlator that should contain the fluctuations that would have otherwise occurred in $\Phi_{semi-classical}$ as it would have been sensitive to the late-time behavior in the CFT.

Chapter 3

Building finite N corrections to HKLL

In this chapter, we shall lay the groundwork to motivate a different way of thinking to instill and perhaps crosscheck finite N corrections we are trying to have built into the prescription by solving for the field near the metric of a wormhole. We choose this metric in particular because of how closely it relates to the cut-off procedure of the large-time behavior of CFT correlators and in a sense gives us a similar result to what one would expect from such an ad-hoc procedure in context to the eternal black holes. Thus it is a natural choice to explain the behavior of finite N corrected theories in the CFT using the HKLL prescription.

3.1 Wormhole Metric

Let us refer to the proposal made by 't Hooft called the “brick wall”. This proposal attempted to explain the entropy of the thermal atmosphere of the particles outside the black-hole horizon as the black hole entropy. In D space-time dimensions the free energy of the thermal gas at temperature T in finite volume V_{D-1} takes the form [5]

$$F = -\pi^{-\frac{D}{2}} \Gamma\left(\frac{D}{2}\right) \zeta(D) T^D V_{D-1} \quad (3.1)$$

The appropriate volume V_{D-1} is defined as the optical metric near the horizon i.e.

$$ds^2 = \sinh^2 y \, ds_{opt}^2 \quad (3.2)$$

and is thus infinite. This meant that the spectrum of field excitations is continuous and the entropy is infinite. To regularise it t'Hooft suggested cutting the region just outside the horizon by introducing a boundary at a small distance ϵ from the horizon and imposing there the Dirichlet boundary condition. This is similar to the cut-off prescription

that was referred to earlier. The brick wall model can be thought of as an artificial way to regularise the otherwise smooth black hole geometry or can be thought of as a crude way to represent the unknown non-perturbative Planckian physics.

Instead, we shall change the near-horizon geometry, and work with a wormhole connecting two asymptotic regions semiclassically separated by horizon. This modification to the black hole geometry would work similarly to the “brick wall” case for both these approaches lead to discrete spectrum and finite entropy, the difference here being that it achieves the same goals but in a smooth way.

Here we first introduce the modified geometry for BTZ black hole.

$$ds^2 = -(\sinh^2 x + \lambda^2(k)) dt^2 + dx^2 + \cosh^2 x d\phi^2 \quad (3.3)$$

The deformation parameter $\lambda(k)$ depends on the large N parameter k and vanishes in the limit $k \rightarrow \infty$. In the classical BTZ black hole, the event horizon is located at $x = 0$, but in the presence of a nonzero λ , this horizon disappears. Instead of a black hole, the resulting geometry takes the form of a wormhole, extending into a second asymptotic region at $x < 0$.

In the classical BTZ description, the regions $x > 0$ and $x < 0$ were separated by the horizon, preventing any direct interaction. However, with the modification, these two regions are now linked by a narrow throat, allowing for information exchange between them. Despite this significant change, the overall spacetime remains asymptotically AdS.

The parameter λ is expected to capture quantum Planck-scale effects, and the curvature at the throat—where the horizon once existed—is of Planckian magnitude. By introducing an appropriate radial coordinate, the metric can be rewritten in a form resembling the standard Schwarzschild metric. $r = r_h \cosh x$

$$ds^2 = -\frac{r^2 - r_h^2 + \lambda^2}{R^2} dt^2 + \frac{R^2}{r^2 - r_h^2} dr^2 + r^2 d\phi^2 \quad (3.4)$$

Now let us solve for the given wormhole metric and thus incorporate the finite N corrections. We first solve for the two-dimensional case to build up the intuition and have some insight on how to tackle higher dimensions.

3.2 Solving for the field in AdS₂

Instead of working with the three-dimensional case, let us instead work with the two-dimensional case, as a direct solution for higher dimensions is rather difficult to obtain, hence the two-dimensional case here can be treated as a warm-up exercise instead, pro-

viding us with an opportunity to learn what we can from the effort.

$$ds^2 = -\frac{r^2 - r_h^2 + \lambda^2}{R^2} dt^2 + \frac{R^2}{r^2 - r_h^2} dr^2 \quad (3.5)$$

where r and r_h is the radial coordinate and the Rindler horizon, and t is the time coordinate.

Using the Ansatz

$$\phi = e^{-i\omega t} \gamma_\omega(r) \quad (3.6)$$

We shall now solve the Klien-Gordon equation:

$$\frac{1}{\sqrt{-g}} \partial_\mu (\sqrt{-g} g^{\mu\nu} \partial_\nu \phi) = m^2 \phi \quad (3.7)$$

$$\frac{1}{\sqrt{-g}} \partial_\mu (\sqrt{-g} g^{\mu\nu} \partial_\nu \phi) - m^2 \phi = 0 \quad (3.8)$$

Here g is the determinant given as

$$g = -\frac{r^2 - r_h^2 + \lambda^2}{r^2 - r_h^2} \quad (3.9)$$

We end up getting the following equation:

$$\begin{aligned} (R^4 \omega^2 - m^2(r^2 - r_h^2 + \lambda^2)) \psi_\omega(r) + ((r^2 - r_h^2)r + (r^2 - r_h^2 + \lambda^2)r) \psi'_\omega(r) \\ + (r^2 - r_h^2)(r^2 - r_h^2 + \lambda^2) \psi''_\omega(r) = 0 \end{aligned}$$

On solving the differential equation we are left with two solutions and remember that the space-time dimension we are working with is 2 we have

$$\begin{aligned} \psi_\omega(r) = C_1 H \left[1 - \frac{\lambda^2}{r_h^2}, \frac{R^2(m(h - \lambda)(h + \lambda) + R^2 \omega^2)}{4r_h^2}, \frac{1}{2}(1 - \Delta), \frac{1}{2}(\Delta), \frac{1}{2}, \frac{1}{2}, \frac{r^2}{r_h^2} \right] \\ + \sqrt{\frac{r^2}{r_h^2}} C_2 H \left[1 - \frac{\lambda^2}{r_h^2}, \frac{r_h^2(2 - mR^2) + (-1 + mR^2)\lambda^2 - R^4 \omega^2}{4r_h^2}, \frac{1}{2}(2 - \Delta), \frac{1}{2}(1 + \Delta), \frac{1}{2}, \frac{1}{2}, \frac{r^2}{r_h^2} \right] \end{aligned}$$

The solution to this differential equation should give us the AdS₂ solution for the Rindler metric under the limit $\lambda \rightarrow 0$, therefore for this limit the solution of the differential equation reduces to

$$\psi_\omega(r) = C_1 L_P \left[(\Delta - 1), \frac{iR^2 \omega}{r_h}, \frac{r}{r_h} \right] + C_2 L_Q \left[(\Delta - 1), \frac{i\omega R^2}{r_h}, \frac{r}{r_h} \right] \quad (3.10)$$

Here, H represents the Huen functions whereas L_P and L_Q represent Legendre Polynomials and Legendre functions respectively. Our job next is to identify the non-normalizable piece (if any) in the above AdS₂ solution. Both these pieces may be normalizable as well.

If we find that the analysis done for AdS₂ for limit $\lambda \rightarrow 0$ is consistent and in agreement with what has already been done. Then it serves as a sanity check and builds our confidence to move further on with the calculations. Think of it as a green light of sorts if you will. This would also allow us to draw parallels between the normalizable pieces and non-normalizable pieces when λ is non-zero, i.e. finite N corrections are in place. Thus making it easier to work with and infer the desired physics.

3.2.1 Sanity Check with known results

Let us find a co-ordinate transform that takes our unmodified metric (without the worm-hole modification) to the one used in [6], which is given as:

$$ds^2 = \frac{L^2}{z^2} \left[-(1 - z^2)d\eta^2 + \frac{1}{(1 - z^2)}dz^2 \right] \quad (3.11)$$

Thus the Klien-Gordon equation is given by:

$$\frac{1}{\sqrt{-g}} \left[\partial_\mu \sqrt{-g} g^{\mu\nu} \partial_\nu \Phi_{\omega t}(z) \right] = m^2 \Phi_{\omega t} \quad (3.12)$$

Let us first calculate the relevant quantities required

$$\begin{aligned} g &= \frac{-L^4}{z^4} \\ g^{\eta\eta} &= -\frac{1}{1 - z^2} \\ g^{zz} &= 1 - z^2 \end{aligned} \quad (3.13)$$

Taking the Anzatz as $\Phi_\omega(z) = \psi(z)e^{-i\Omega}$, let us work on K-G equation.

$$\begin{aligned} \frac{z^2}{R^2} \partial_\eta \left[\frac{R^2}{z^2} g^{\eta\eta} \partial_\eta \Phi_\Omega(z) \right] + \frac{z^2}{R^2} \partial_z \left[\frac{R^2}{z^2} g^{zz} \partial_z \Phi_\Omega(z) \right] &= \frac{M^2 \Phi_\Omega(z)}{z^2} \\ \frac{\Omega}{R^2(1 - z^2)} \psi(z) + \frac{1}{R^2} \partial_z \left[(1 - z^2) \partial_z \psi(z) \right] &= \frac{M^2 \psi(z)}{z^2} \end{aligned} \quad (3.14)$$

Now let us use the following co-ordinate transformation to bring this equation to our coordinate system.

$$\begin{aligned} z &= \frac{r_h}{r} & dz &= -\frac{r_h}{r^2} dr & dz^2 &= \frac{r_h^2}{r^4} dr^2 \\ \eta &= \frac{r_h t}{R^2} & d\eta &= \frac{r_h}{R^2} dt & d\eta^2 &= \frac{r_h^2}{R^4} dt^2 \end{aligned} \quad (3.15)$$

Thus the metric transform as:

$$\begin{aligned}
 ds^2 &= \frac{R^2}{z^2} \left[- (1 - z^2) d\eta^2 + \frac{1}{1 - z^2} dz^2 \right] \\
 ds^2 &= \frac{R^2 r^2}{r_h^2} \left[- \left(1 - \frac{r_h^2}{r^2} \right) \left(\frac{r_h^2}{R^4} dt^2 \right) + \left(\frac{1}{1 - \frac{r_h^2}{r^2}} \right) \frac{r_h^2}{r^2} dr^2 \right] \\
 ds^2 &= \frac{R^2 r^2}{r_h^2} \left[\left(-\frac{r^2 - r_h^2}{r^2} \right) \left(\frac{r_h^2}{R^4} dt^2 \right) + \left(\frac{r^2}{r^2 - r_h^2} \right) \frac{r_h^2}{r^2} dr^2 \right] \\
 ds^2 &= -\frac{r^2 - r_h^2}{R^2} dt^2 + \frac{R^2}{r^2 - r_h^2}
 \end{aligned} \tag{3.16}$$

This is the metric that we are working with thus we have the correct transformation, for further checks let us try to transform a known from equation to the differential equation in our coordinates.

E.O.M in z and η coordinates.

$$\begin{aligned}
 \frac{1}{\sqrt{\frac{R^4}{z^4}}} \left[\partial_\eta \left(\sqrt{\frac{R^4}{z^4}} g^{\eta\eta} \partial_\eta \Phi(z, \eta) \right) + \partial_z \left(\sqrt{\frac{R^4}{z^4}} g^{zz} \partial_z \Phi(z, \eta) \right) \right] &= (\Delta^2 - \Delta) \Phi(z, \eta) \\
 \frac{\Omega}{R^2(1 - z^2)} \psi(z) + \frac{1}{R^2} \partial_z [(1 - z^2) \partial_z \psi(z)] &= \frac{M^2 \psi(z)}{z^2}
 \end{aligned} \tag{3.17}$$

Performing the coordinate transformation for the η we have

$$\begin{aligned}
 \Phi(z) &= e^{-i\Omega\eta} \psi(z) & \frac{\partial t}{\partial \eta} &= \frac{R^2}{r_h} \\
 \Phi(r, t) &= e^{-i\Omega \frac{r_h^2}{R^2} t} \psi(r) \\
 \frac{\partial \Phi}{\partial \eta} &= -i\Omega \frac{r_h}{R^2} \frac{\partial t}{\partial \eta} e^{-i\Omega \frac{r_h^2}{R^2} t} \psi(r) \\
 \frac{\partial}{\partial \eta} \left(\frac{\partial \Phi}{\partial \eta} \right) &= -i\Omega \frac{r_h^2}{R^2} (-i\Omega) \frac{R^2}{r_h} e^{-i\Omega \frac{r_h^2}{R^2} t} \psi(r) \\
 \frac{\partial^2 \Phi}{\partial \eta^2} &= -\Omega^2 e^{-i\Omega \frac{r_h^2}{R^2} t} \psi(r)
 \end{aligned} \tag{3.18}$$

Performing the coordinate transformation for the z we have:

$$\begin{aligned}
 \frac{\partial \Phi}{\partial z} &= \frac{\partial r}{\partial z} \frac{\partial \Phi}{\partial r} \\
 \frac{\partial \Phi}{\partial z} &= -\frac{r^2}{r_h} \frac{\partial \Phi}{\partial r} \\
 \frac{\partial r}{\partial z} \frac{\partial}{\partial r} \left[\frac{\partial r}{\partial z} (1 - z^2) \frac{\partial \Phi}{\partial r} \right] &= -\frac{r^2}{r_h} \left(\frac{\partial}{\partial r} \left[\frac{r^2 - r_h^2}{r^2} \left(-\frac{r^2}{r_h} \frac{\partial \Phi}{\partial r} \right) \right] \right) \\
 \frac{\partial r}{\partial z} \frac{\partial}{\partial r} \left[\frac{\partial r}{\partial z} (1 - z^2) \frac{\partial \Phi}{\partial r} \right] &= \frac{r^2}{r_h^2} \frac{\partial}{\partial r} \left[(r^2 - r_h^2) \frac{\partial \Phi}{\partial r} \right]
 \end{aligned} \tag{3.19}$$

Considering that $\Omega = \frac{R^2\omega}{r_h^2}$ Therefore the differential equation becomes:

$$\begin{aligned} \left(\frac{r^2}{r^2 - r_h^2}\right) (\Omega^2 \psi(r)) + \frac{r^2}{r_h^2} \left[\frac{\partial}{\partial r} (r^2 - r_h^2) \frac{\partial \psi}{\partial r} \right] &= \frac{r^2}{r_h^2} (\Delta^2 - \Delta) \psi(r) \\ \omega^2 R^4 \psi(r) + (r^2 - r_h^2) \partial_r \left([r^2 - r_h^2] \frac{\partial \psi(r)}{\partial r} \right) &= (\Delta^2 - \Delta) (r^2 - r_h^2) \psi(r) \end{aligned} \quad (3.20)$$

The required solution is:

$$\psi(r) = C_1 L_P \left[(\Delta - 1), \frac{iR^2\omega}{h}, \frac{r}{h} \right] + C_2 L_Q \left[(\Delta - 1), \frac{i\omega R^2}{h}, \frac{r}{h} \right] \quad (3.21)$$

The differential equation transforms exactly to our differential equation and thus the solutions match as required, this serves as a foundation for the coordinate transformation between our Differential Equation and already known Differential Equations is consistent and thus we use this as check that when the λ parameter goes to zero that is the wormhole modification is not present our solution to known solutions [6] in such a limiting case. Let us now transform the λ corrected metric as well, we have:

$$ds^2 = \frac{r^2 - r_h^2 + \lambda^2}{R^2} dt^2 + \frac{R^2}{r^2 - r_h^2} dr^2 \quad (3.22)$$

Performing the coordinate transformation we get:

$$ds^2 = \frac{R^2}{z^2} \left[- (1 - z^2 + \gamma^2 z^2) d\eta^2 + \frac{dz}{1 - z^2} \right] \quad (3.23)$$

where γ is the rescaled parameter which goes as $\frac{\lambda}{r_h}$.

When we take this metric and solve for the equation of motion for the massless case we get the following result:

$$\psi[z] = C_1 \cosh \left[\frac{\sqrt{1 - z^2} \Omega \wp[\arcsin[z], 1 - \gamma^2]}{\sqrt{-1 + z^2}} \right] - i C_2 \sinh \left[\frac{\sqrt{1 - z^2} \Omega \wp[\arcsin[z], 1 - \gamma^2]}{\sqrt{-1 + z^2}} \right] \quad (3.24)$$

Here, \wp refers to the Elliptic functions for the γ corrected massless case. Next we draw parallels with γ or λ going to zero case, in order to identify the Normalisable piece.

3.2.2 Finding the normalizable piece for Massive fields for $\lambda = 0$

Now let us perform a thorough analysis of the solutions presented such that we may learn how to do deal with and identify the normalizable piece from the solutions we get, From the above equations we have:

$$\psi(r) = C_1 L_P \left[(\Delta - 1), \frac{iR^2\omega}{h}, \frac{r}{h} \right] + C_2 L_Q \left[(\Delta - 1), \frac{i\omega R^2}{h}, \frac{r}{h} \right] \quad (3.25)$$

From this let us expand each individual expression in terms of known hypergeometric functions in order to extract the normalizable piece.

$$C_2 L_Q \left[(\Delta - 1), \frac{i\omega R^2}{h}, \frac{r}{h} \right] = \left[\frac{r}{r_h} \right]^{-\Delta} e^{-\frac{\pi R^2 \omega}{r_h}} \frac{\Gamma \left(\Delta + \frac{iR^2 \omega}{r_h} \right)}{\Gamma \left(\Delta + \frac{1}{2} \right)} \sqrt{\pi} \left(\frac{r^2}{r_h^2} - 1 \right)^{\frac{iR^2 \omega}{r_h}} {}_2F_1 \left[\frac{\Delta + \frac{iR^2 \omega}{r_h} + 1}{2}; \frac{\Delta + \frac{iR^2 \omega}{r_h}}{2}; \Delta + \frac{1}{2}; \frac{r_h^2}{r^2} \right] \quad (3.26)$$

which is comparable to what is already known for AdS_2 massive case, alas it is unfortunate that for λ modified metric for massive case, we get the Huen functions which are not very good to work with, and are a dead end as of now, since these functions are rather archaic, although if the reader has any knowledge of the said functions please do reach out so that I may learn from you with any insight you may have on the said topic.

3.3 Massless fields for $\lambda = 0$

Furthermore moving on to the massless case for $\lambda = 0$ we get the solutions to be

$$y[r] = C_1 \cos \left[\frac{R^2 \omega \operatorname{arctanh} \left(\frac{r}{r_h} \right)}{r_h} \right] - C_2 \sin \left[\frac{R^2 \omega \operatorname{arctanh} \left(\frac{r}{r_h} \right)}{r_h} \right] \quad (3.27)$$

Here it is evident that the normalisable piece is the Sin function as it vanishes as $r \rightarrow \infty$ which again matches with established results from known calculations. This serves as a strong foundation to stand upon when we introduce λ non-zero case for the massless fields.

Chapter 4

An Analytic journey through the wormhole metric

4.1 Bulk reconstruction

Our main aim in this chapter is to now show the rigorous calculations carried out in the same vein as Chapter 2. We will analytically tackle the massless AdS₂ case such that we can weave the λ corrected metric to define the ad-hoc cut-off in the CFT side. Furthermore, we shall try to corroborate a rough estimate of λ and show that it is consistent with other studies and estimates of it so far.

$$ds^2 = -\frac{r^2 - r_h^2 + \lambda^2}{R^2} dt^2 + \frac{R^2}{r^2 - r_h^2} dr^2 \quad (4.1)$$

Let us again define a tortoise coordinate such that

$$dr^* = \frac{R^2}{\sqrt{(r^2 - r_h^2)(r^2 - r_h^2 + \lambda^2)}} \quad (4.2)$$

Parametrize: $\frac{r_h}{r} = \sin u$

Therefore,

$$\begin{aligned} r^* &= R^2 \int_{\infty}^r \frac{dr}{\sqrt{(r^2 - r_h^2)(r^2 - r_h^2 + \lambda^2)}} \\ &= \frac{R^2}{r_h^2} \int_{\infty}^r \frac{dr}{\sqrt{\left(\frac{r^2}{r_h^2} - 1\right) \left(\frac{r^2}{r_h^2} - 1 + \frac{\lambda^2}{r_h^2}\right)}} \\ &= -\frac{R^2}{r_h^2} \int_0^{\sin^{-1}(\frac{r_h}{r})} \frac{r_h \csc^2 u \cos u}{\sqrt{(\csc^2 u - 1)(\csc^2 u - 1 + \frac{\lambda^2}{r_h^2})}} du \\ &= -\frac{R^2}{r_h} \int_0^{\sin^{-1}(\frac{r_h}{r})} \frac{du}{\sqrt{1 - m \sin^2 u}} \rightarrow \mathbf{EllipticF} \end{aligned} \quad (4.3)$$

$$= -\frac{R^2}{r_h} \text{EllipticF} \left(\sin^{-1} \frac{r_h}{r}, \sqrt{1 - \frac{\lambda^2}{r_h^2}} \right) \quad (4.4)$$

Note: When $r \rightarrow r_h$ we may analytically continue our solution to the complete Elliptic Function.

For $r \rightarrow r_h$

$$\int_0^{\frac{\pi}{2}} \frac{du}{\sqrt{1 - \frac{\lambda^2}{r_h^2} \sin^2 u}} = K \left(\sqrt{1 - \frac{\lambda^2}{r_h^2}} \right) \quad (4.5)$$

Now let us use Bulk Reconstruction to write the field in terms of the Boundary operator. The calculation will follow exactly how it was done in Chapter 2.

On Solving the Klien-Gordon equation we get the following solution for the field.

$$\Phi(r, t) = (C_1 \cos(\omega r^*) + C_2 \sin(\omega r^*)) e^{-i\omega t} \quad (4.6)$$

where, $r^* \rightarrow$ tortoise coordinate. As $r \rightarrow \infty$, $r^* \rightarrow \frac{r_h}{r}$

Therefore the field at the boundary becomes:

$$\begin{aligned} \lim_{r \rightarrow \infty} f(r) &\approx \left(\frac{R^2}{r} \right) a_\omega \\ C_2 &= -\frac{a_\omega}{\omega} \end{aligned} \quad (4.7)$$

Therefore the mode solution will be:

$$\begin{aligned} \Phi(r, t) &= -\frac{1}{\sqrt{2\pi}} \int_{-\infty}^{\infty} d\omega \left(e^{-i\omega t} f_\omega(r) \frac{a_\omega}{\omega} + h.c \right) \\ &= \frac{1}{2\pi} \int_{-\infty}^{\infty} \int_{-\infty}^{\infty} d\omega dt \left(e^{-i\omega(t-t')} \sin \left(-\frac{\omega R^2}{r_h} E_f \left[\sin^{-1} \left(\frac{r_h}{r} \right), \sqrt{1 - \frac{\lambda^2}{r_h^2}} \right] \right) \right) \frac{O(t')}{\omega} \end{aligned} \quad (4.8)$$

Therefore we may identify the Kernel as:

$$K(r, t) = -\frac{1}{2\pi} \int_{-\infty}^{\infty} \frac{e^{-i\omega(t-t')}}{\omega} \sin(-\omega r^*) d\omega \quad (4.9)$$

This is exactly the kind of Kernel we had in Chapter 2, which yields the $Sgn(x)$ function on further evaluation, therefore:

$$K(r, t) = \frac{1}{4} (Sgn[t - t' + r^*] - Sgn[t - t' - r^*]) \quad (4.10)$$

which has support over $t' \in [t - r^*, t + r^*]$ Thus any bulk point can be written as follows:

$$\begin{aligned}\Phi(t, r) &= \frac{1}{2} \int_{t-r^*}^{t+r^*} O(t') dt' \rightarrow \lambda \text{ corrections} \\ \Phi(t, r) &= \frac{1}{2} \int_{t-\delta t}^{t+\delta t} O(t') dt' \rightarrow \mathbf{KL's way}\end{aligned}\tag{4.11}$$

Compared to what was done in Chapter 2 we see that the form of the bulk point remains the same and that the finite N corrections that were weaved into the metric are now present in the limits of the above integral by the virtue of the Kernel, which what we had expected initially. The spread of the integral is encoded in r^* which also contains the t_{cut} naturally just as we were hoping it would.

4.2 Estimation of λ

From the previous analysis done in the initial chapters, we could conjure a guess estimate for λ which should be of the order of $e^{-\frac{S}{\Delta}}$. This is strongly motivated by the size of the excision and as was shown in this paper [7]. Now we shall try and derive the estimate of λ thus, to do this we need to first evaluate at what distance from the horizon do the corrections come into play given that this should be similar to how close we can go towards the horizon before the finite N corrections start to make a difference we have:

$$\delta t = \frac{R^2}{r_h} \log \frac{r + r_h}{r - r_h}\tag{4.12}$$

This is the same calculation as was done in equation (2.30) onwards with the constants preserved this time thus, the extent to which we can probe using λ correction is:

$$r = r_h \left(1 + 2e^{-\frac{S}{2\Delta}}\right)\tag{4.13}$$

Since this extent of r is calculated using t_{max} we may now calculate the rough estimate of λ as well using the expression for the tortoise coordinate $r^*(r)$

$$\begin{aligned}r^*(r) &= -\delta t + \frac{\lambda^2}{8r_h^2} \left(-\frac{rR^2}{r_h^2 - r^2} - \frac{R^2}{2r_h^2} \log \frac{r + r_h}{r - r_h} \right) \\ &= -\delta t - \frac{\lambda^2}{8r_h^2} \left(-\frac{rR^2}{r^2 - r_h^2} + \delta t \right) \\ &= -\delta t - \frac{\lambda^2}{8r_h^2} \left(-\frac{r_h(1 + 2e^{-\frac{S}{2\Delta}})R^2}{r_h^2(1 + 4e^{-\frac{S}{2\Delta}} + 4e^{-\frac{S}{\Delta}} - 1)} + \delta t \right) \\ &= -\delta t - \frac{\lambda^2}{32r_h^2} \left(-\frac{(e^{\frac{S}{2\Delta}} + 2)R^2}{4r_h e^{-\frac{S}{2\Delta} + 1}} + \delta t \right)\end{aligned}\tag{4.14}$$

Since $e^{-\frac{S}{2\Delta}} \ll 1$ we may write:

$$\begin{aligned} &= -\delta t - \frac{\lambda^2}{32r_h^2} \left(-\frac{(e^{\frac{S}{2\Delta}} + 2)(1 - (e^{-\frac{S}{2\Delta}})R^2)}{r_h} + \delta t \right) \\ &= -\delta t - \frac{\lambda^2}{32r_h^2} \left(-\frac{(2 \sinh \frac{S}{2\Delta} - e^{-\frac{S}{2\Delta}} + 1)R^2}{r_h} + \delta t \right) \end{aligned} \quad (4.15)$$

Now we compare our limits with what we had in Chapter 2, considering that both formalisms are to be treated on equal footing we have:

$$\begin{aligned} t_{cut} &= t - r^* \\ t - r^* &= t - \delta t + t_{max} \end{aligned} \quad (4.16)$$

Near $r \approx r_h$; $\delta t = t_{max}$, now substituting for all the values of the variables above we get:

$$\begin{aligned} -t_{max} &= \frac{\lambda^2}{32r_h^2} \left(\left((-2 \sinh \frac{S}{2\Delta} - e^{-\frac{S}{2\Delta}} + 1) \frac{R^2}{r_h} + t_{max} \right) \right. \\ \lambda^2 &= -\frac{32r_h^2 t_{max}}{\left(\left((2 \sinh \frac{S}{2\Delta} - e^{-\frac{S}{2\Delta}} + 1) \frac{R^2}{r_h} + t_{max} \right) \right)} \\ \lambda^2 &= \frac{16r_h^2 S}{\Delta \left(2 \sinh \frac{S}{2\Delta} - e^{-\frac{S}{2\Delta}} + 1 - \frac{S}{2\Delta} \right)} \end{aligned} \quad (4.17)$$

Considering large S we can make some more approximations.

$$\lambda^2 = \frac{4r_h^2 S e^{-\frac{S}{2\Delta}}}{\Delta} \quad (4.18)$$

Now since we have an estimate for λ we may now use it's value to write down the value of $r^*(r)$ therefore we have:

$$r^*(r_h) = -\delta t + \frac{R^2 S}{2\Delta r_h} \quad (4.19)$$

Therefore the modified field now with the wormhole metric will be

$$\begin{aligned} \Phi_{mod}^{WH}(t, r) &= \frac{1}{2} \int_{t+r^*}^{t-r^*} dt' O(t') \\ &= \frac{1}{2} \int_{t+\frac{R^2 S}{2\Delta r_h}}^{t+\delta t - \frac{R^2 S}{2\Delta r_h}} dt' O(t') \end{aligned} \quad (4.20)$$

Again the form of the equation is the same as before, interestingly enough in our quest to get a natural cutoff for late-time behavior in the CFT, we are also given a symmetric cut-off by the wormhole metric. Perhaps this is to preserve the light-cone structure/support that is dropped on the boundary by the bulk point. For our case now we shall only focus on the upper limit of the integral and compare it with what KL had worked out.

$$\frac{1}{2} \int_{t-\delta t}^{t+\delta t - \frac{R^2 S}{2\Delta r_h}} O(t') = \frac{1}{2} \int_{t-\delta t}^{t+\delta t} O(t') - \frac{1}{2} \int_{t+\delta t - \frac{R^2 S}{2\Delta r_h}}^{t+\delta t} O(t') \quad (4.21)$$

Now we may draw parallels to the calculations done in Chapter 2 again:

$$\Phi_{WH}(r, t) = \Phi_{semiclassical}(r, t) - \Phi_{ex}(r_{ex}, t_{ex}) \quad (4.22)$$

with $t' \in [t + \delta t, t + \delta t - \frac{R^2 S}{2\Delta r_h}]$ Therefore

$$\begin{aligned} t_{ex} &= \frac{t_{cut} + t + \delta t}{2} \\ \delta t_{ex} &= \frac{t + \delta t - t_{cut}}{2} \end{aligned} \quad (4.23)$$

using what we have got using the wormhole metric we can calculate the estimate for t_{ex} and δt_{ex} and hence compare it with known results

$$\begin{aligned} t_{cut} &= t - r^* \\ t_{ex} &= t + \delta t - \frac{R^2 S}{4\Delta} \\ \delta t_{ex} &= \frac{R^2 S}{4\Delta} \\ r_{ex} &= R \coth \frac{RS}{2\Delta r_h} \end{aligned} \quad (4.24)$$

Thus we see that all the quantities that have been excised have a contribution from the λ , which is expected since λ is of the order of the fluctuations that were expected even though they may not arise in the Rindler horizon due to it's infinite S and thus in turn infinite N behavior. This analysis helps us establish how these corrections might look in a different system. Furthermore, the behavior is in line with what the finite N treatment of HKLL tells us during the correlator calculation which we will see now. But before that let us talk about the excised region a little more, in essence noting changes as:

$$\begin{aligned} \tanh \frac{r_h t}{R^2} &= \frac{2RT}{R^2 + T^2} \\ Z_{ex} &= 2Re^{-\frac{S}{2\Delta}} \end{aligned} \quad (4.25)$$

Thus the only change that takes place is in the comparable position of the excised field and thus in turn of the new field inserted,

$$\begin{aligned} \Phi_{WH}(r, t) &= \Phi_{BTZ}(r, t) - \Phi_{semi-classical}(t_{ex}, r_{ex}) \\ &= \Phi_{BTZ} - \Phi_{semi-classical} \left(\frac{R^2 S}{4\Delta}, R \coth \frac{RS}{2\Delta r_h} \right) \end{aligned} \quad (4.26)$$

4.3 Correlator

Now let us calculate the bulk to boundary correlator and see if we can recover the finite N corrected behavior, i.e. correlator with a cut-off. We shall use the same CFT two-point function as before:

$$\langle O_R(t') O_R(t'') \rangle = \frac{1}{2} \int_{t-\delta t + \frac{R^2 S}{2\Delta r_h}}^{t+\delta t - \frac{R^2 S}{2\Delta r_h}} dt' \frac{1}{1 - \cosh(t' - t'')} \quad (4.27)$$

Thus the correlator will be

$$\begin{aligned} \langle \Phi_{WH}(r, t) O_R(t') \rangle &= \frac{1}{2} \int_{t-\delta t + \frac{R^2 S}{2\Delta r_h}}^{t+\delta t - \frac{R^2 S}{2\Delta r_h}} dt' \langle O_R(t') O_R(t'') \rangle \\ &= \frac{1}{4} \left(\coth \frac{t + \delta t - \frac{R^2 S}{2\Delta r_h} - t''}{2} - \coth \frac{t - \delta t + \frac{R^2 S}{2\Delta r_h} - t''}{2} \right) \end{aligned} \quad (4.28)$$

Again using the Hyperbolic trig identities we have:

$$\langle \Phi_{WH}(r, t) O_R(t') \rangle = \frac{1}{2} \left(\frac{\sinh(\delta t - \frac{R^2 S}{2\Delta r_h})}{\cosh(\delta t - \frac{R^2 S}{2\Delta r_h}) - \cosh t - t''} \right) \quad (4.29)$$

Note that \sinh term is always negative as $\delta t \lesssim \frac{R^2 S}{2\Delta r_h}$ which is t_{max} similarly the denominator is also negative hence it nets out a plot in the positive quadrant that decays similar to how the correlator decayed in the ad-hoc treatment.

Chapter 5

Future Outlook and Conclusion

5.1 Conclusion

Following the extensive discussions presented in the preceding sections, an important question arises: why not apply the HKLL prescription directly to finite N without resorting to modifications such as the wormhole modification? This is a crucial point that deserves careful consideration. The standard HKLL prescription, when applied to finite N , encounters significant difficulties due to the behavior of the kernel. Specifically, the kernel, which is essential for reconstructing bulk operators in terms of CFT data, diverges when attempting to perform the integral. This divergence presents a fundamental obstruction to directly implementing the HKLL procedure in this context.

As explored in earlier sections, the late-time behavior of the CFT correlator exhibits characteristics that are incompatible with the requirements of the HKLL prescription. Ideally, for a well-defined bulk reconstruction, one would expect the correlator to decay smoothly over time. However, at finite N , the correlator instead undergoes persistent fluctuations, preventing the necessary cancellations that would otherwise eliminate divergences in the kernel. This problem necessitates the introduction of a corrective mechanism to restore consistency to the reconstruction procedure.

There are two primary ways to address this issue. One approach is to impose an ad-hoc cut-off at a later time t_{max} , which effectively regulates the integral by eliminating contributions from times beyond this threshold. While this method is operationally simple, it lacks a fundamental justification and appears to be an artificial modification rather than an intrinsic feature of the theory. The second approach, which is the focus of this thesis, is to modify the bulk metric itself to incorporate finite N corrections naturally. This method has the advantage of embedding the required modifications directly into the structure of spacetime, thereby providing a more consistent and theoretically motivated framework for bulk reconstruction at finite N . We showed rigorous calculations to support our claims while drawing parallels with already established results by Kabat and

Lifschytz, we were able to recover the exact behavior we were hoping for in the Rindler AdS_2 case and the t_{cut} did indeed manifest itself much more naturally to the point that it was even symmetric in the limit.

Furthermore, since our results align with well-established results for massless case, we can be reasonably confident in the validity of our approach. In particular, our calculations, when subjected to an appropriate coordinate transformation, reduce to known differential equations. This provides additional reassurance that our methodology is on the right track and that our modifications to the reconstruction procedure are capturing essential features of finite N effects in the bulk. Not only this it also allows us to be confident in our approach to applying this methodology for the 3-dimensional BTZ black hole, which would be the next step naturally, work on the same is underway as of now.

5.2 Future Outlook

Since the case of $\lambda = 0$ along with the 2 dimensional AdS_2 case was thoroughly analyzed and cross-checked against existing results, we will now turn to investigate the more general scenario where $\lambda \neq 0$ in AdS_3 . This represents a significant step forward in understanding the interplay between finite N effects and bulk reconstruction.

Through this analysis, we aim to gain a more comprehensive understanding of how finite N CFT correlators behave at large times. This includes studying how the smearing function adapts to modifications in the bulk metric and how these modifications manifest in the kernel that maps bulk operators to the CFT boundary for 3-dimensional theory now. A key objective of this work has been to find a physically motivated justification for the ad-hoc cut-off imposed on CFT correlators at finite N . A deeper understanding of this issue could provide new perspectives on the role of finite entropy corrections in holography and offer insights into the broader framework of bulk reconstruction.

Additionally, our results have the potential to shed light on Planck-scale physics near the black hole horizon. The physics of near-horizon regions remains a critical area of research, with important implications for quantum gravity, black hole information, and holography. Understanding how finite N corrections influence near-horizon physics could provide valuable clues about the nature of black hole microstates and the fundamental structure of spacetime. Furthermore, our findings may contribute to ongoing discussions about wormhole modifications of the near-horizon metric. Depending on the results of further analysis, we may either reinforce the necessity of such modifications or propose alternative interpretations based on our reconstruction framework. We also hope to apply our studies to the stretched horizon model and understand how the wormhole metric differs from the stretched horizon.

Overall, while numerous challenges remain, this study represents a meaningful step

toward unraveling the complexities of bulk reconstruction at finite N . We remain optimistic that further exploration of these ideas will yield new insights and open up exciting directions for future research in quantum gravity and holography.

References

- [1] A. Hamilton, D. Kabat, G. Lifschytz and D. Lowe, “Holographic representation of local bulk operators,” *Phys. Rev. D* **74**, 066009 (2006) doi:10.1103/PhysRevD.74.066009 [arXiv:hep-th/0606141 [hep-th]]. 502 citations counted in INSPIRE as of 26 Sep 2024
- [2] R. Bousso, “A Covariant entropy conjecture,” *JHEP* **07**, 004 (1999) doi:10.1088/1126-6708/1999/07/004 [arXiv:hep-th/9905177 [hep-th]]. 949 citations counted in INSPIRE as of 22 Nov 2024
- [3] L. Susskind and E. Witten, “The Holographic bound in anti-de Sitter space,” [arXiv:hep-th/9805114 [hep-th]]. 934 citations counted in INSPIRE as of 22 Nov 2024
- [4] D. Kabat and G. Lifschytz, “Finite N and the failure of bulk locality: Black holes in AdS/CFT,” *JHEP* **09**, 077 (2014) doi:10.1007/JHEP09(2014)077 [arXiv:1405.6394 [hep-th]]. 34 citations counted in INSPIRE as of 22 Nov 2024
- [5] S. Solodukhin, “Restoring unitarity in BTZ black hole,” *Phys. Rev. D* **71**, 064006 (2005) doi:10.1103/PhysRevD.71.064006 [arXiv:hep-th/0501053 [hep-th]]. 55 citations counted in INSPIRE as of 22 Nov 2024
- [6] P. Dey and N. Kajuri, “Bulk reconstruction and Bogoliubov transformations in AdS₂,” *JHEP* **09**, 170 (2021) doi:10.1007/JHEP09(2021)170 [arXiv:2106.07304 [hep-th]].
- [7] C. Germani and D. Sarkar, *Fortsch. Phys.* **64**, 131-143 (2016) doi:10.1002/prop.201500057 [arXiv:1502.03129 [hep-th]].